Synthesis of Nano Particles against Hep-G-2 Cancer cell line

Hala Moustafa Ahmed[1].Mohamed Sameeh Abo-Shanab[2]
Medical Biophysics-Biomedical Equipment Department[1]-Radiology Department[2]-Faculty of applied medical sciences
October 6 University

ABSTRACT:-

Gold nanoparticles (GNPs) are excellent tools for cancer cell imaging and basic research. However, they have yet to reach their full potential in the clinic. Gold nanoparticles (GNPs) have been used to improve cellular targeting and sensitization. In this paper, we explored the mechanism of GNP enhanced or inhibition sensitivity resistant Hep-G-2 cells. Proliferation and cell survival were measured using MTT assay, and western blotting was used to determine the expression of p53 and cyclin proteins that correlated to cell cycle regulation. GNPs showed a 1.5–2.0 fold enhancement in growth inhibition when compared to C.T alone. At present, we are only beginning to understand the molecular mechanisms that underlie the biological effects of GNPs, including the structural and functional changes of cancer cells. Comparing the cell cycle change, G2/M arrest was accompanied by decreased expression of cyclin A and p53, and increased expression of cyclin E and cyclin B1.GNPs accumulation of cells in the G2/M phase and induced acceleration in the G0/G1 phase at 15.3% versus 28.4% for controls at 36 hours. GNPs trigger activation of the CDK kinases leading to cell cycle acceleration in the G0/G1 phase and accumulation in the G2/M phase.

Keywords:Hep-G-2, Gold Nanoparticles(GNPs), Imaging.

INTRODUCTION:-

Nanotechnology is in the spotlight of therapeutic innovation [1], and GNPs are particularly promising tools to improve cancer treatment [2]. Due to their unique optical properties, non-toxic nature, relatively simple preparation and functionalization, GNPs are excellent candidates for many biological applications, such as imaging, drug delivery and photothermal therapy.These applications commonly take advantage of the particles' strong light scattering, intense absorption, and electromagnetic field enhancement that result from localized surface plasmon resonance [3, 4].

Many antimicrobial agents are limited in clinical applications, because of their poor membrane penetration, complications and side-effects especially at higher doses and relatively higher incidence of bacterial infection due to growing resistance of bacteria to conventional antibiotics and due to in judicial use of many antibiotics.[5] So the use of nanomaterials is being increasingly applied for medical uses and is of great interest as an approach to killing or limiting the activity of numerous micro-organisms. [6].

Colloidal gold is a suspension (or colloid) of nanometer-size particles of gold in a fluid, usually water. The liquid is usually either an intense red color (for particles less than 100 nm) or blue/purple (for larger particles) [7]. Due to the unique optical, electronic, and molecular-recognition properties of gold nanoparticles, they are the subject of substantial research, with applications in a wide variety of areas, including electron microscopy, electronics, nanotechnology, and materials science. The generation of colloidal gold nanoparticles was first described by Michael Faraday in 1857 when he described the synthesis of multicolored solutions by reacting gold chloride with sodium citrate. In cancer research, colloidal gold can be used to target tumors and provide imaging and detection; these gold nanoparticles are surrounded with Raman reporters, which provide light emission that is over 200 times brighter than quantum dots, gold nanoparticles accumulate in tumors, due to the leakiness of tumor vasculature, and can be used as contrast agents for enhanced imaging [8].

(GNPs) showed significantly increased cellular uptake compared to neutral nanoparticles [9]. Cytoplasmic uptake of Glu-GNP followed by 2 Gy of ortho-voltage irradiation resulted in significant growth inhibition in cancer cells. GNPs showed a 1.5–2.0 fold enhancement in growth inhibition when compared to GNPs alone. Although we have demonstrated that GNPs can significantly enhance radio sensitivity in prostate cancer treatment the mechanism of this enhancement has not been thoroughly investigated. [10].

Aim of the work:-

The main objective of this work is to find GNPs the control Hep-G-2 cell growth .We investigated the effects of GNPs on cell cycle regulation.

MATERIALS AND METHODS:-

1-Biophysical method- Synthesis of Gold nanoparticles (GNPs):-

The GNPs were characterized using transmission electronic microscopy (TEM), Kratos Axis 165 x-ray photoelectron spectroscopy (XPS) and ICP-MS (Kratos Analytical) as described previously [10]. Shape and Size of colloidal Gold nanoparticle deter-

mine by TEM performed on JEOL JEM-2100 high resolution transmission electron microscope at an accelerating voltage of 200 kV, respectively (Table.1)

Table 1. Properties of colloidal Gold nanoparticle

GNPs	Gold
Appearance (Color)	**Gradate Pink**
Appearance (Form)	**Liquid**
Solubility	**Water Soluble**
Avg. Size	**5 nm diameter**
Shape	**Spherical shape**

TEM analysis allows accurate measurement of particles average diameter results are shown in table (1). UV – Spectroscopy was used in the characterization of GNPs. The results shown in figure (1-A). The prepared gold NPs show that UV-Vis absorption spectrum exhibited a single Plasmon band at 520 nm, indicative to formation of spherical gold NPs. TEM micrograph had been imaged by VACSERA for Photo-Electronics clearly and shows that, the prepared gold NPs has spherical diameter is ranging between 16 ± 5 nm.

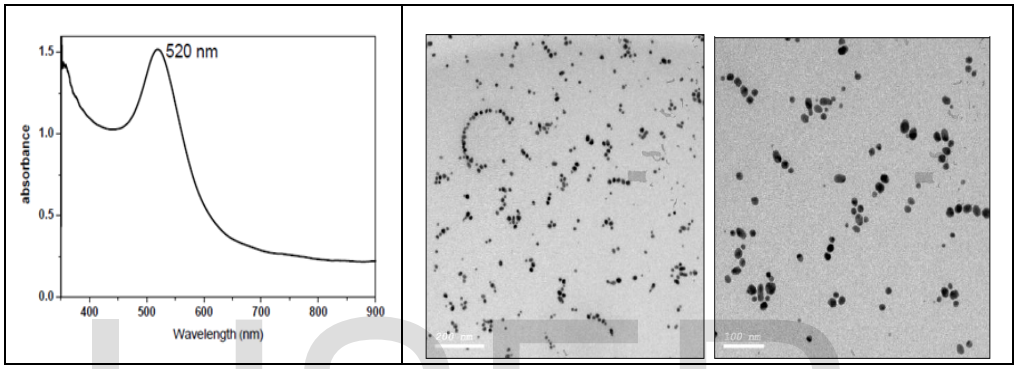

Fig: (1)- (A) Absorption Spectrum of Au NPs -(B) TEM micrograph of GNPs

In order to calculate the concentration of GNPs in solution, refer to Beer Lambert's Law (Swineheart, D. F.).

$$A = \epsilon\, c\, f$$

Where the product of molar absorptivity (ϵ), molar concentration (c), and the path length (b) equals to absorbance, two attenuating species will exist in the solution (gold (III) chloride trihydrate and trisodium citrate dihydrate) [11]. Therefore, the absorbance of the GNP ($AGNP$) would be represented by:

$$A_{GNP} = A_1 + A_2 = \epsilon_1 c_1 f + \epsilon_2 c_2 f$$

Where the sum of the absorbance of trisodium citrate dihydrate (A_1) and the absorbance of gold (III) chloride trihydrate (A_2) in the solution is equal to the absorbance of the GNPs. Then solve for the concentration of gold (III) trihydrate in the solution. Solve for the amount of moles gold in the solution and then multiply by Avogadro's number to determine how many particles were produced in the synthesis [12] . The amount of atoms to form a nanoparticle (N) with diameter (d) would be represented by:

$$N = \frac{\pi \rho d^3}{6M}$$

Where one must consider both density of gold (ρ), molar mass of gold (M), and the diameter in nanometers (d).By knowing how many gold atoms consist of a single GNP, one can determine how many GNPs are formed in the solution by taking the quotient of GNPs in solution by number gold atoms to produce a single atom. One then can calculate the concentration of the solution by dividing the number of nanoparticles by the volume of the solution. Another approach to determining the concentration of GNPs in solution would to assume that the entire reducing agent has been used up and only one attenuating species exist in solution, the GNPs. The absorbance of the GNPs would be represented by:

$$A_{GNP} = \epsilon_{GNP} c_{GNP} f$$

Where $cGNP$ represents the concentration of the GNPs and ϵGNP would be represented as the molar absorptivity of the GNPs .Referring to Figure 1, use the absorption at the Surface Plasmon Resonance (SPR) peak for the absorption of the GNPs to solve for the concentration of gold nanoparticles. The extinction coefficient for GNPs have an SPR peak at a wavelength of 515-520 nm was obtained from Sigma-Aldrich. To determine the path length (f), the path length of the cuvette was used in the Perkin Elmer Lambda 35 UV/Vis spectrophotometer. Using equation ($AGNP = \epsilon GNP\ cGNPf$), solve for the concentration of GNPs in the solution. With the volume of the sample and molarity, the moles of the GNPs can be calculated. With the total number of GNPs in solution, find the concentration by dividing it by the volume of solution .With the moles of GNPs, multiply it by Avogadro's number to get

the total number of GNPs in the solution [13]. In order to determine the average diameter, the diameter of a GNP (*d*) can be represented by:

$$d = e^{(B_1 \frac{A_{spr}}{A_{450}} - B_2)}$$

By knowing the absorption at the SPR peak and 450 nm, an estimate of the GNPS can be determined if the particles are between 5 to 80nm.

2- Cell lines and culture:-

The Hep-G-2 cell culture was purchased from VACSERA, EGYPT. The cell lines were maintained in Roswell Park Memorial Institute 1640 medium (RPMI-1640) (Gibco) supplemented with 10% bovine calf serum (Hyclone) or 10% Fetal Bovine Serum (Hyclone), 2 mM L-glutamine, 100 units/ml penicillin and 100 mg/ml streptomycin (Cellgro) in a humidified atmosphere of 5.2 % CO_2 at 37°C.The medium was replaced with fresh medium (RPMI-1640) three times per week until the cells grew 80–90% confluence. The plates were then incubated overnight at 37°C in a 5.2% CO_2 humidified environment. Cell lines at final density of 1×10^5 cells/mL were cultured in 24-well plates (300 µL per cell) for the MTT assay. The cells were exposed to different concentrations (0.025ml-0.05ml-0.1ml) (GNPs) using 46 KV and 5 mAs in x-ray image anterior posterior (AP) for 36 hours. The final concentration of GNPs nanoparticles was 100 µg/ ml dissolved in Phosphate Buffered Saline (PBL). Control group was cultivated without GNPs on the same conditions.

3-Uptake assay:-

When the cells reached 70% confluence, the target cells were exposed to the vehicle, or 15 nM GNPs at 37°C. All assays were performed in triplicate. After 12, 24 and 36 hours of incubation, the free GNPs in the cell cultures were removed by washing the plated cells twice with the PBS buffer. The number of cells was counted with a hemocytometer. Two ml of 20% HNO_3 was added to each sample to lyse the cells. The gold mass in each solution was measured using inductively coupled plasma mass spectrometry (ICP-MS). The number of gold nanoparticles GNPs was calculated via the gold mass, and the number of GNPs in the lysis solution was divided by the number of cells to yield the number of GNPs taken up per cell [14].

4-MTT assay for cell viability:-

After all samples were cultured for 36 hours, 20 µL of 5 g/L-3-(4, 5-dimethythiazol- 2-yl)-2, 5-diphenyl tetrazolium bromide (MTT) was added. It was then incubated for additional 4 hours. Then, the plates were centrifuged at 1000 rpm for 10 minutes, the supernatant was discarded lightly, after which 150 µL of Dimethyl sulphoxide (DMSO) was added into each well followed by gentle shaking in the shaker incubator at 37°C for 15 min. The optical density (OD) was recorded at 492 nm on micro plate reader (I mark™). To determine whether GNPs enhanced the sensitivity of Hep-G-2 cells to GNPs, cells were treated with GNPs alone. Untreated control samples were arbitrarily assigned a value of 100% and the results of all treatments were normalized to the control group. The cell growth inhibitory rate was calculated by the following formula:

Inhibatory Rate =1-average O.D nm of treated group/average O.D nm of control group x100%

5-Statistical Analysis:-

Continuous variables were recorded as mean ± SD; ANOVA-f test, followed by Tukey's test, was used to evaluate the significance of difference ($P < 0.05$) among group. Data analysis was made by Fisher's exact and Pearson's correlation tests. Data were expressed as mean ± standard error (S.E). Using SPSS for Widows (Chicago, II, USA) when appropriate $p < 0.05$ was considered statistically significant. Histogram analysis combines techniques that compute statistics and measurements based on the gray-level intensities of the image pixel. The Student's t-test and other statistical analysis were performed using statistical SPSS -12 programs.

Results and discussions:-

1-Fluoroscopic x-ray:

Using a fluoroscopic x-ray machine (Philips Duo-diagnostic code RDXR001) 46 Kv and 5 mAs, was used to image the synthesized phantom before and after the injection of nanoparticles into it. The Hounsfield unit (HU) scale used in measurement is a linear transformation of the original linear attenuation coefficient measurement in one in which the radio density of distilled water at standard pressure and temperature (STP) is defined as zero Hounsfield units (HU), while the radio density of air at STP is defined as -1000 HU. Thus, a change of one Hounsfield unit (HU) represents a change of 0.1% of the attenuation coefficient of water since the attenuation coefficient of air is nearly zero. (Table .2) shows Hounsfield measurement for the three samples of nanoparticles with different concentration.

In summary for the experimental results, by using fluoroscopic x-ray machine for scanning the phantom with different concentration of GNPs samples vary (0.01 ml ,0.05ml,0.025 ml), and performing Hounsfield measurements on the samples. Since HU measure the attenuation coefficient, It note that the HU measurement as shown in (table.2) start with a value of 537 nm at GNPs concentration of 0.1 ml and start to decrease gradually until it reach a value of 474 nm at GNPs concentration of 0.025 with an attenuation percentage from the 1st sample of -8.4%.

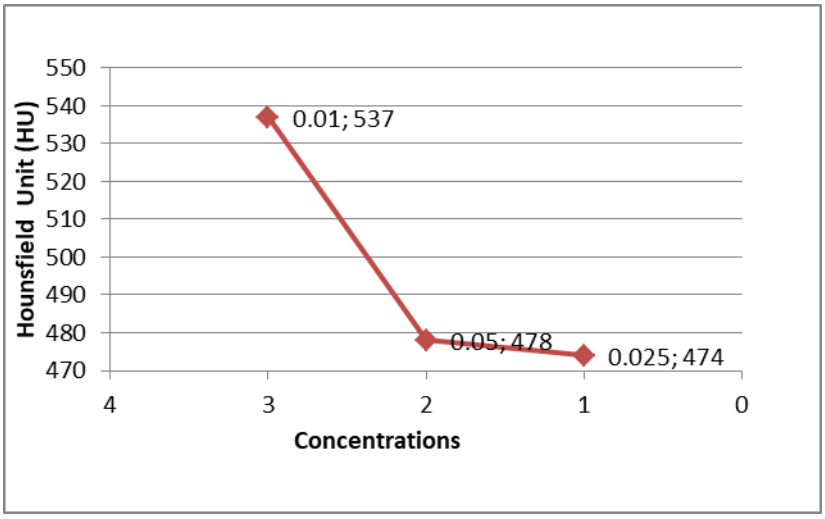

Figure 2. Measured HU with different concentration of GNPs in (AP) X-ray images using 46 Kv and 5 mAs.

Figure .2 shows a 2D representation of the results obtained from Fig .1 and table.2.In conclusion for the experimental results, the reason for decreasing the HU measurement (attenuation decreasing) by decreasing the concentration is that when the concentration decrease the distance between GNPs increase and the electromagnetic coupling (electric field) between them decrease, to prove that a computational analysis and finite element simulation will be performed using CST STUDIO program.

3-Determination of Gap Distance between GNPs:-

The concentrations of the sample and volume of single GNPs, We can determine the gap distance between two neighboring GNPs ,since the radios of a single GNPs which is (2.5 nm) , so the distance determined , by multiply volume of a single GNPs by the density of each sample we get the mass of a single GNPs , by dividing the total mass by the mass of a single GNPs we get the total number of GNPs in each concentration in cm^3 .Calculate the gap distance between GNPs for different concentrations .So after calculating the total number of GNPs in each concentration in cm^3. Taking the cubic root we get the number of GNPs in a one cm^3.Taking the inverse of the number of GNPs in a one cm we get the space between GNPs in cm units. Multiplying this space by 10^7, we get the space between GNPs in nm units of the three concentrations (0.1ml, 0.05ml, and 0.025ml) a gap distance (S) between GNPs calculated as shown in (Table 2).

Table 2. Change of Hounsfield for different concentration of GNPs and its attenuation percentage

HU of GNPs	Concentrations	Attenuation %	Gap distance (S) between GNPs(nm)
537	0.01		23
478	0.05	-5.9%	30
474	0.025	-6.3%	37

4-Electric Field Simulation for the three Concentrations:-

The simulation of electric field (EF) intensity at both the gap distance (S) between GNPs and at the edges of GNPs for the three concentrations according to the change of gap distances (s) (23, 30, and 37 nm), .Study the relation between gap distance change due concentrations change and the EF intensity values which effect on the X-ray diagnoses.

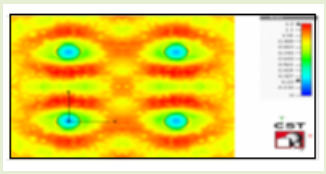

A

B

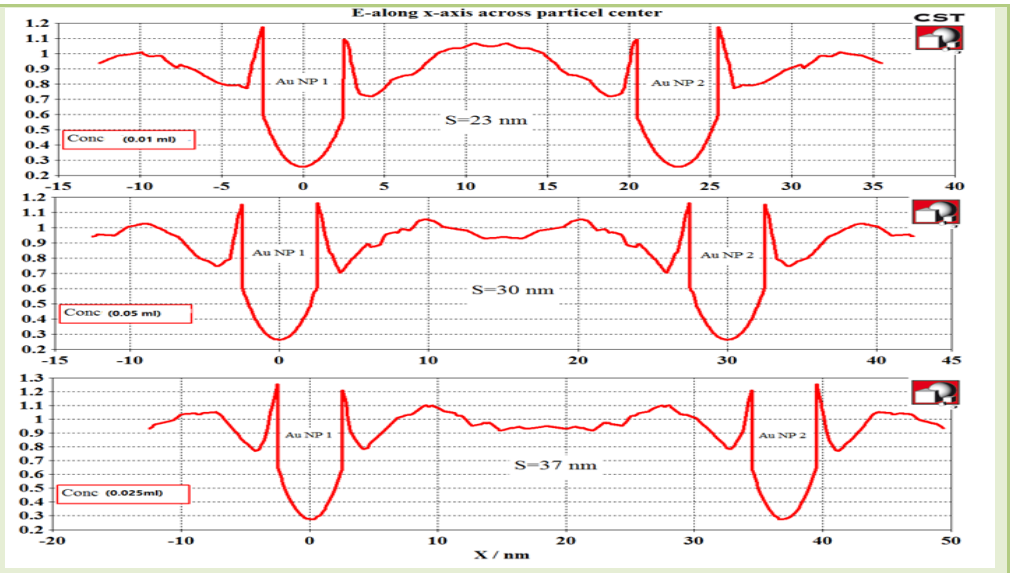

C

Figure (3)-(A) Show EF intensity distribution, (B) Show 3D EF intensity,(C) Show the 2D Electric field (EF) intensity in different concentrations (0.01ml.0.05ml and 0.025ml) .

From figure (3) which represent the EF intensity distribution on the gap distance between GNPs and on the outer and inner edges of them for the three concentrations of GNPs, the following results noted by decreasing the concentrations the gap distances (S) increases gradually from (23 nm) at concentration (0.01ml), to (30 nm) at concentration (0.05ml) until it reach (37 nm) at concentration (0.025ml). The multipacks electric field at the gap distance decreases gradually from (1.0475V/m) at concentration (0.01ml), to (0.9368 V/m) at concentration (0.05ml) until it reach (0.9478 V/m) at concentration (0.025ml).The EF at the inner edges of GNPs fluctuated during the three concentrations between (1.0885 V/m), (1.1190V/m) and (1.1399V/m).The EF at the inner edges of GNPs fluctuated during the three concentrations (1.1513 V/m) (1.1372V/m) and (1.12518V/m).The average of EF intensity of all EF value (midpoint ,outer edges of GNPs 1, inner edges of GNPs 1, outer edges of GNPs 2,and inner edges of GNPs 2) have value =1 V/m.

5-Distribution and uptake of GNPs on Hep-G-2 cells:-

GNPs, that are synthesized by binding gold nanoparticles (GNPs, 10.8 nm) the average number of GNPs associated with each cell was (2.06 ± 0.24)×10^4 for naked GNPs, and (7.3±0.66)×10^4 for GNPs (figure 4). After exposure to 15 nM GNPs for 12,24 and 36 hours, the average numbers of GNPs taken up by each Hep-G-2 cell per time interval are illustrated in (figure 5). The average number of GNPs increased with time and peaked at 4 hours at (8.04 ± 0.29) × 10^4.

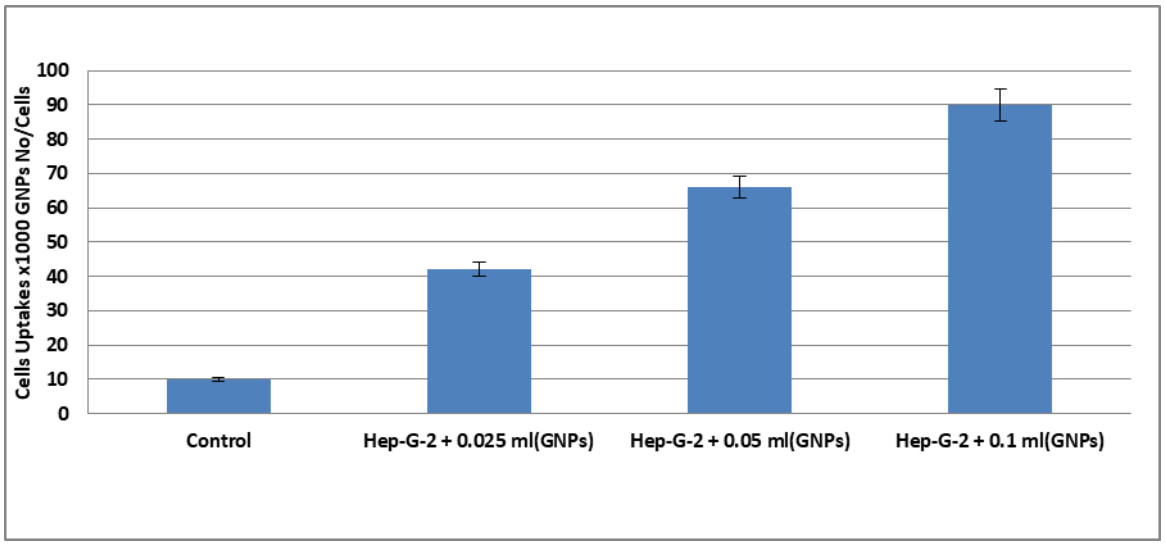

Figure 4. Nanoparticle (GNPs) distribution and uptake on Hep-G-2 cells at 4 hours

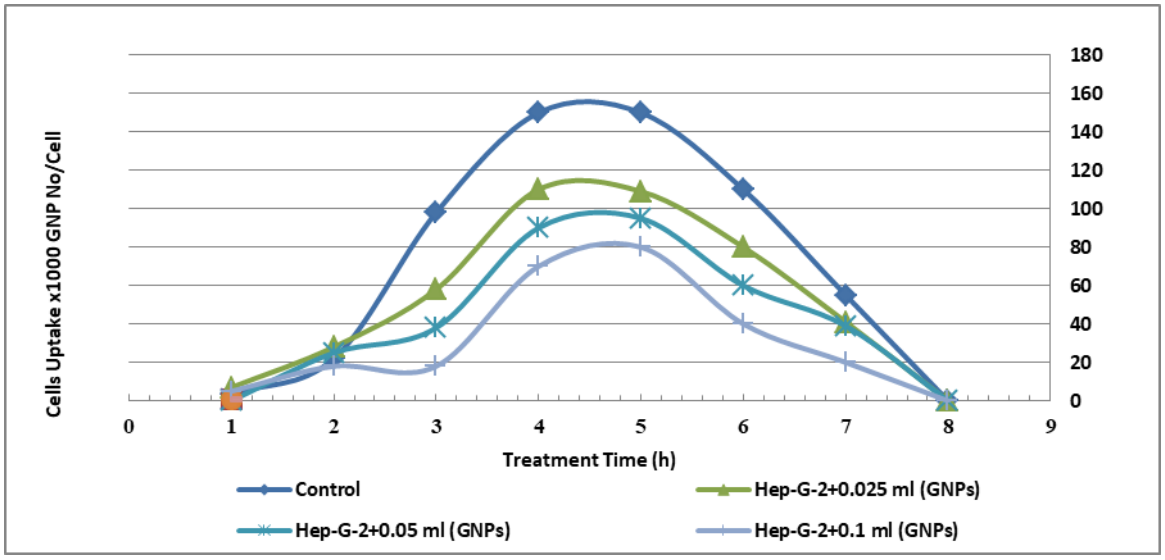

Figure 5. Nanoparticle (GNPs) distribution and uptake on Hep-G-2 cells at dynamic cell uptakes over 36 hours

6- GNPs enhanced radiation sensitivity:-

At 36 hours, GNPs induced inhibition of cell proliferation of 10.2%, 7.4%, 6.2%, respectively. However, the combination of GNPs inhibited cell proliferation in Hep-G-2 cells by 22.8% ($P < 0.005$) (figure 6).The dose-dependent effects induced by various concentrations of GNPs are shown in (figure 7).

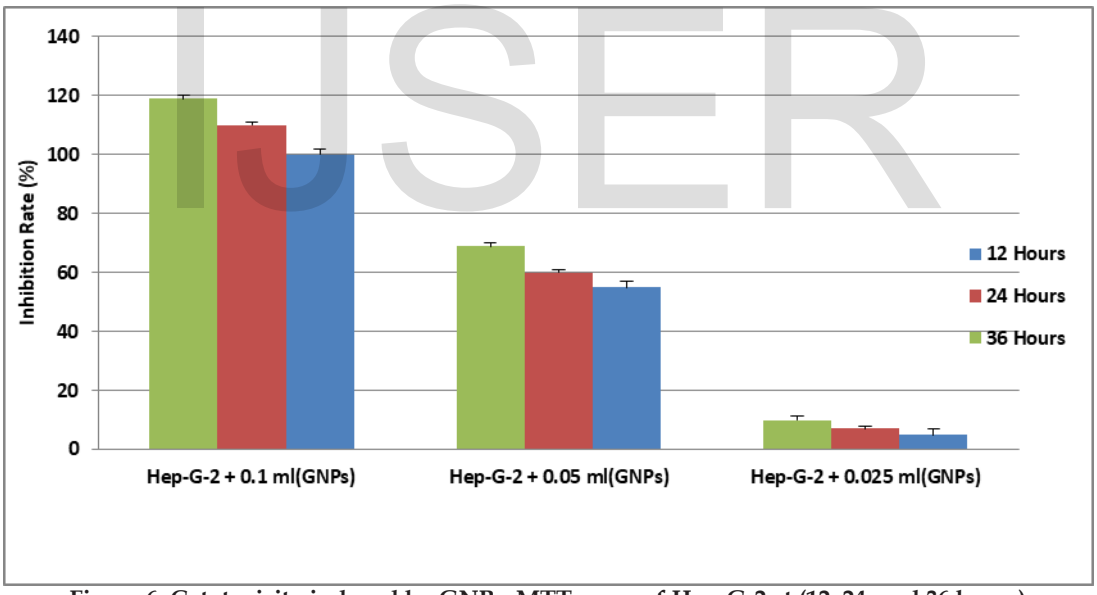

Figure 6. Cytotoxicity induced by GNPs, MTT assay of Hep-G-2 at (12, 24, and 36 hours)

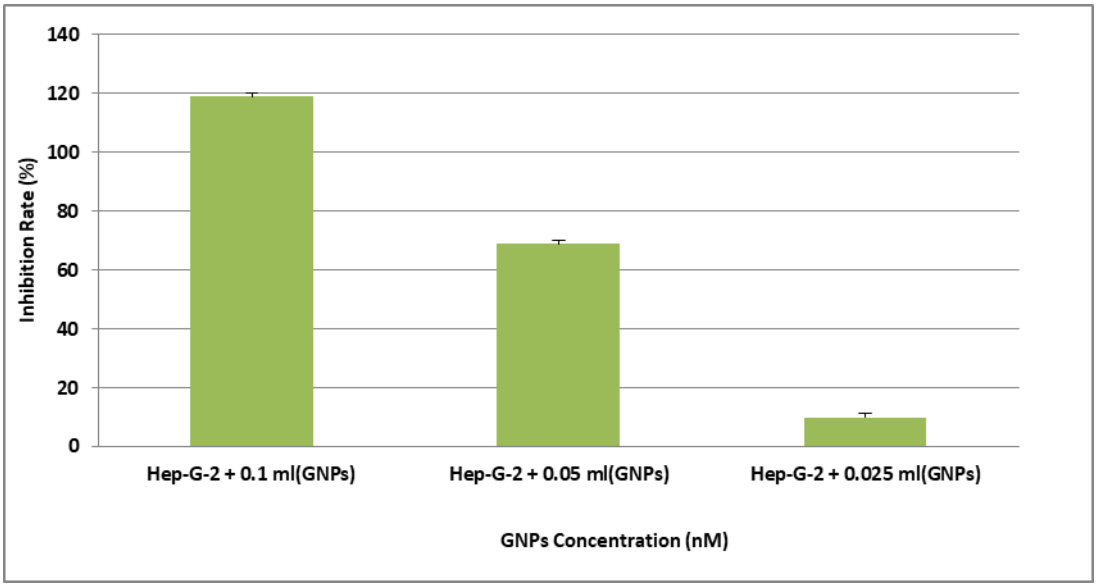

Figure 7. The dose-dependent effects induced by various concentrations of GNPs at 36 hours

7- GNPs do not enhance the sensitivity of non-cancerous cells to GNPs:-

To assess potential effects on Hep-G-2 cells treated with GNPs. Both groups had comparable growth rates. (Figures 8 and 9) demonstrate that GNPs induced 26.8% , 12.7% and 8.4% inhibition rates in the Hep-G-2 cell viabilities, respectively. Following 2 hours incubation with GNPs, the cell viability of Hep-G-2 cells was further decreased, with a inhibition rate.

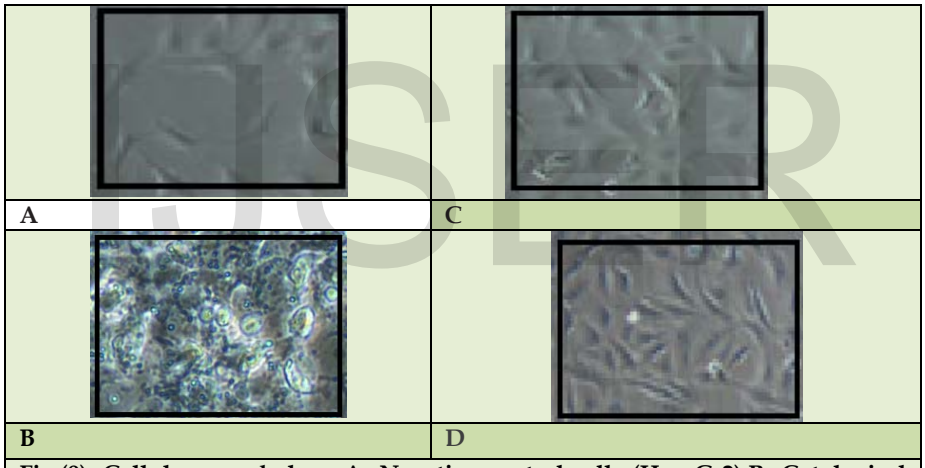

Fig.(9): Cellular morphology-A- Negative control cells (Hep-G-2).B- Cytological changes in (Hep-G-2) cell lines +0.1 ml GNPs after 72 hours cells that were swollen, refractile and distinct from transparent cell sheet .C- Hep-G-2 +0.05 ml GNPs after 72 hours .Hep-G-2 cells growth (minimal).D- Hep-G-2, +0.025 ml GNPs after 72 hours Cells spindle shape,no evidance of morphological cellular damage.

In figure (9) where the cytological changes (90% CPE) could be detected within 72 hours post viral inoculation Fig. 9-(C&D) compared with the negative control .The delayed detection of cytological changes may be attributed to the low viral load in collected specimens, recording 90% CPE on the 72 hours post infection. Alternating passaging in cell culture could be a supporting factor to maximize the viral load, where on the 5th passage the cytological changes could be detected within 2-4 days post viral infection showed a gradual increase in the mean viral infectivity titer relatively to time.

8- Changes in cyclins in GNP mediated cell cycle arrest:-

The cell samples were analyzed by western blotting using specific antibodies against the activated cyclin B1, cyclin A and cyclin E proteins that are involved in either CDK1 or CDK2 kinases. GNPs activated proteins for both kinases as follows. Cyclin B1/CDC2 is an important kinase for the regulation of the G2 to M transition [15].Figures (10) indicate GNPs induced a significant increase in the expressible cyclin B1 intensity (1.9 fold in 24 h, and 1.6 fold in 48 h, respectively). After treatment with 0.01 ml GNPs plus Hep-G-2 cells, the expression of cyclin B1 was increased by 8.0 fold at 24 hours and 1.7 fold at 48 h when compared to the control. [16] Cyclin A regulates at least two CDKs, CDK1 and CDK2, and is believed to be necessary for progression through the S phase and the G2–M transition [17]. After treatment with either 0.05 ml GNPs plus Hep-G-2 cells, the expressible intensities of cyclin A were at 24 h significantly reduced by 84.5% with GNPs plus Hep-G-2 cells. Combined 0.0025 ml GNPs plus Hep-G-2 cells resulted in a 97.7% inhibition of cyclin A protein at 24 h.[19] Cyclin E is a G1 cyclin that has been shown to be one of the key regula-

tors of the G1–S transition [18]. Cyclin E binds to CDK2, forming the cyclin E/CDK2 complex, which pushes the cell from the G1 to the S phase (G1/S transition). GNPs increased the expression of cyclin E by 1.2 fold at 24 hours and by 1.5 fold at 48 h.

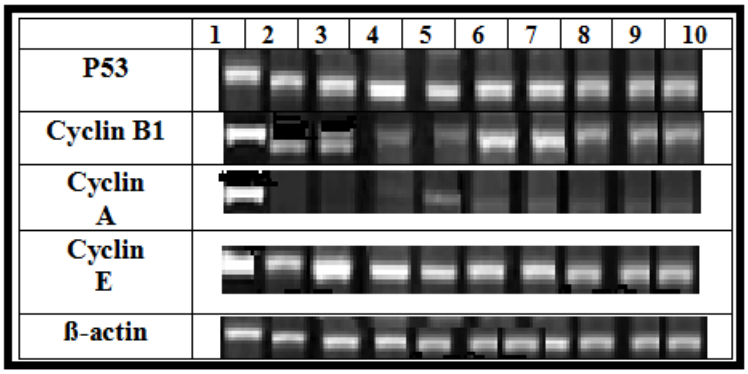

Figure 10. (A) Western blot of protein expressions of p53, cyclin B1, cyclin A and cyclin E induced by GNPs with Hep-G-2 (Lane 1: control; lane 2:GNPs at 12 h; lane 3:GNPs at 24 h; lane 4: GNPs at 36 h; lane 5: GNPs at 12 h; lane 6 GNPs at 24 h; lane 7: GNPs at 36 h; lane 8: GNPs at 12 h; lane 9 GNPs at 24 h; lane 10: GNPs at 36 h.

Figure 10 shows a significantly increased expression of cyclin E and cyclin B1, and decreased expression of cyclin A. Cyclin E is a G1 cyclin that has been shown to be one of the key regulators of the G1–S transition. Cyclin E binds to CDK2, forming the cyclin E/CDK2 complex, which pushes the cell from the G1 to the S phase (G1/S transition) [19].GNPs inhibited expression of cyclin E to accelerate the G0/G1 phase and in turn to accumulate cells in the G2/M phase. After GNP treatment, the expression of cyclin B1 by DU-145 cells was significantly increased ($P < 0.05$). The increase in cyclin B1 results from cell accumulation in the G2/M phase.[20] Therefore, cell accumulation in the G2/M phase induced by GNPs is different from cell arrest in the G2/M phase induced by DNA damage. DNA damage induces increased
p53 expression to inhibit cyclin B1 expression and cause cell arrest in the G2/M phase. In this study, GNPs inhibited p53 expression, resulting in cyclin E overexpression, which shortens the G1/S transition. Furthermore, GNPs induced cell accumulation in the G2/M phase via the acceleration of the G0/G1 phase. Increased cyclin B1 expression is a marker of cell accumulation in the G2/M phase.[21] One function of p53 is to decompose cyclin B1. When the expression of p53 was inhibited by GNPs, a weaker decomposability induced accumulation of cyclin B1. As an S phase complex, the major function of cyclin A is to regulate the S phase. [23] However, cyclin A/CDK2 has also been implicated in mitosis [22].Microinjection of cyclin A/CDK2 can promote mitotic entry of human G2 phase cells. Conversely, the injection of cyclin A specific antibodies after the S phase prevented human cells from progressing through mitosis,[24]-[25].

Conclusion:-

Nanoparticles (GNPs) were synthesized by Biophysical method and electric field measurements were presented of metal gold nanoparticle at three different concentrations prove that the contrast agent GNPs can be used for the noninvasive. The combination of (GNPs) nanoparticles and Hep-G-2 was found to be more effective than activity of the Hep-G-2 cells individually. The electric field intensity at the midpoint between neighboring GNPs decreases gradually due to increases of the gap distances between them due to the decreases of the concentration. In this study, GNPs inhibited cyclin A expression by 42.3%. Cyclin A along with CDK2 forms the cyclin A–CDK2 complex, which initiates the G2/M transition. Inhibition of cyclin A induced a delay of the G2/M transition.

References:-

1. Wright J. Nanotechnology: Deliver on a promise. Nature. 2014; 509: S58-S9.
2. Ghosh P, Han G, De M, Kim CK, Rotello VM. Gold nanoparticles in delivery applications. Adv Drug Del Rev. 2008; 60: 1307-15.
3. Hutter E, Maysinger D. Gold nanoparticles and quantum dots for bioimaging. Microsc Res Tech. 2011; 74: 592-604.
4. Hutter E, Maysinger D. Gold-nanoparticle-based biosensors for detection of enzyme activity. Trends Pharmacol Sci. 2013; 34: 497-507.
5. M. Rai, A. Yadav and A. Gade, *Biotechnol. Adv.*, 2009, 27, 76.
6. S. Prabhu and E. K Poulose, *Intl. Nano Lett.*, 2012, 2, 3.
7. A. M. Fayaz, K. Balaji, M. Girilal, R. Yadav, P. T.Kalaichelvan and R. Venketesan, *J. Nanomed.: Nanotechol.,Bio. and Med.,* 2010, 6, 103.
8. R.Varshney, S. Bhadauria and M. S. Gaur, *Adv. Mat. Lett.*,2010, 1, 232.
9.Kong T *et al* 2008 Enhancement of radiation cytotoxicity inbreast-cancer cells by localized attachment of gold nanoparticles *Small* 4 1537–43
10. Zhang X *et al* 2008 Enhanced radiation sensitivity in prostate cancer by gold-nanoparticles *Clin. Invest. Med.* 31 E160–7
10.Kong T *et al* 2008 Enhancement of radiation cytotoxicity in breast-cancer cells by localized attachment of gold nanoparticles *Small* 4 1537–43
11.Turkevich, John, Cooper P Stevenson and James Hillier. "A Study of the Nucleation and Growth Processes in the Synthesis of Colloidal Gold." *Discussions of the Faraday Society* (1951): 55-75.
12.Lu, Yan; Wang, Lixia; Chen, Dejun; Wang, Gongke. "Determination Of the Concentration and

the Average Number of Gold Atoms in a Gold Nanoparticle by Osmotic Pressure." *Langmuir* (2012): 9282-9287. Journal.

13.Haiss, Wolfgang; Nguyen T. K., Thanh; Aveyard, Jenny; Fernig G., David. "Determination of Size and Concentration of Gold Nanoparticles from UV−Vis Spectra." *Analytical Chemistry* (2007): 4215-4221. Journal.
14.Kong T *et al* 2008 Enhancement of radiation cytotoxicity in breast-cancer cells by localized attachment of gold nanoparticles *Small* 4 1537–43
15. S´anchez I and Dynlacht B D 2005 New insights into cyclins, CDKs, and cell cycle control *Sem. Cell Dev. Biol.* 16 311–21
16. Zou H, McGarry T J, Bernal T and Kirschner M W 1999 Identification of a vertebrate sister-chromatid separation inhibitor involved in transformation and tumorigenesis *Science* 285 418–22
17. Reimann J D *et al* 2000 Emi1 is a mitotic regulator that interacts with Cdc20 and inhibits the anaphase-promoting complex *Cell* 105 645–55.
18.PaganoM *et al* 1992 Cyclin A is required at two points in the human cell cycle *EMBO J.* 11 961–71
19. Iliakis G and Nusse M 1983 Evidence that repair and expression of potentially lethal damage cause the variations in cell survival after x irradiation observed through the cell cycle in Ehrlich ascites tumor cells *Radiat. Res.* 95 87–107
20. Sanford K K and Parshad R 1999 The contribution of deficient DNA repair to chromosomal radiosensitivity of CHO cells after G2 irradiation *Cancer Genet. Cytogenet.* 108 38–41
21. Bandara L R *et al* 1992 Cyclin A recruits p33CDK2 to the cellular transcription factor DRTF1 *J. Cell Sci. (Suppl)* 16 77–85
22. Goldstone S *et al* 2001 Cdc25-dependent activation of cyclin A/CDK2 is blocked in G2 phase arrested cells independently of ATM/ATR *Oncogene* 20 921–32
23. PaganoM *et al* 1992 Cyclin A is required at two points in the human cell cycle *EMBO J.* 11 961–71
24.Ke, S.; Zhou, T.; Yang, P.; Wang, Y.; Zhang, P.; Chen, K.; Ren, L.; Ye, S. :Gold nanoparticles enhance TRAIL sensitivity through Drpl-mediated apoptotic and autophagic mitochondrial fission in NSCLC cells. Int. J. Nanomed. 2017, 12, 2531–2551.
25.Hainan Sun 1, Jianbo Jia 1,2 ID , Cuijuan Jiang 3 and Shumei Zhai 1 :Gold Nanoparticle-Induced Cell Death and Potential Applications in Nanomedicine Int. J. Mol. Sci. 2018, 19, 754; doi:10.3390/ijms19030754